

# Observation of low-depolarization contrails at Florence (Italy) using a 532-1064 nm polarization LIDAR

Massimo Del Guasta

Istituto Ricerca sulle Onde Elettromagnetiche CNR, Florence, Italy

Kandula Niranjan

Dept. of Physics, Andhra University, Visakhapatnam, India

**Abstract.** Contrail backscatter and polarization measurements made using a 532-1064 nm LIDAR in Florence (Italy) indicated that, in most of the cases, the contrail depolarisation and color ratio resemble the usual cirrus. In 20% of the cases, a depolarisation below 15% was observed, both in isolated contrails and in cirrus-embedded contrails. In a few cases, a very low depolarisation, down to 3%, was observed at temperatures in the  $-40^{\circ}$  to  $-65^{\circ}$  C range. In two measurements, a low depolarization was coupled with a high color ratio in the 2-4 range. The low-depolarisation, high color ratio contrail observations are discussed in the light of the results of recent T-matrix scattering simulations. The two events lasted at least 10-20 minutes in the LIDAR data, suggesting a very slow growth or no growth at all of the initial micron-sized contrail particles in the large ice crystals typical of cirrus.

## 1. Introduction

Microphysical properties of contrails have been the focus of study in recent years because of their potential impact on climate through direct and indirect radiative forcing. It is believed that, during the primary stage of contrail formation, large numbers of ice crystals are nucleated which subsequently grow in size. Heymsfield et al. (1998) reported that the contrail core, in fact, acted as a source of ice crystals, and that the periphery acted as a growth region when the environment provided a continuous source of vapour. Contrails are distinguished from natural cirrus in their tendency to remain thin and to generate strong laser backscattering and depolarisation (Sassen and Hsueh, 1998). Some observations have been made in order to characterize the microphysical properties of the contrails by using polarization LIDAR at a visible wavelength (usually 532 nm). By using a scanning depolarisation LIDAR, Freudenthaler et al. (1996) reported a depolarisation ratio of 10% for contrails younger than 1.6 minutes at  $T \leq -60^{\circ}$  C, and higher values of up to 50% at later times. Low values were attributed to near spherical liquid or frozen particles, or to particles much smaller than the LIDAR wavelength: an increase in depolarisation indicated particle growth. Mishchenko and Sassen (1998), using improved T-matrix computations (Mishchenko et al., 1996), have shown that ice crystals with effective radii as small as several tenths of a micron can produce depolarisations that exceed 50% at visible wavelengths, which explains the high depolarisation observed even in young contrails. Sassen and Hsueh (1998) reported that linear depolarisation ratios were higher than 10% even in the

youngest contrails, with typical values of between 30% and 70% in the older ones. Preliminary observations made using a dual wavelength (0.532 and 1.064  $\mu\text{m}$ ) polarization LIDAR at IROE (Florence, Italy) have at times shown low-depolarisation contrails lasting more than 10 minutes. These events triggered a long measurement campaign in which the depolarisation and the backscatter color ratio of contrails were investigated. Results are reported here, and are discussed in terms of contrail microphysics in the light of recent results of scattering simulations carried out on spheroidal particles.

## 2. Methods

The LIDAR was operated in Florence (Italy,  $43^{\circ}\text{N}$ ), a town located under a busy air corridor. The zenith-pointing system, which derives from the one described by Stefanutti et al., (1992), operated at 532 nm (300 mJ, linearly polarized) and 1064 nm (400 mJ, circular polarization) with a repetition rate of 10 Hz. The receiver was a 80 cm Cassegrain telescope with a field of view of 1 mrad. The radiation at 1064 nm was detected by an APD, while 532 nm radiation was analysed in polarization and detected by two PMTs. A LeCroy digitizer with a 75-m resolution was used for the acquisition of all three channels. LIDAR signals were averaged over a period of 1 minute. LIDAR data processing followed the procedure described by Morandi (1992) and Del Guasta et al. (1993) in order to obtain calibrated vertical-backscatter profiles. Daily time-height-backscatter plots were produced, from which contrail events were identified with the help of visual and web-cam observations.

Presumed contrails were identified in the plots on the basis of the limited vertical extent and of the marked backscatter (compared with the surrounding cirrus). The web-cam shots, when available, confirmed the presence of the contrail. This procedure is safe in the case of isolated contrails, but could be erroneous in the case of cirrus-embedded ones: the enhanced backscatter produced by thin layers of horizontally-oriented ice plates within cirrus could be erroneously attributed to contrails. We estimate this ambiguity to be present in about 10% of the cirrus-embedded contrail cases reported in this work.

Each contrail event was re-processed separately. The depolarisation ratio:

$$\delta = \frac{\beta_{532s}}{\beta_{532p} + \beta_{532s}}$$

and the color ratio:

$$R = \frac{\beta_{532p} + \beta_{532s}}{\beta_{1064}}$$

profiles were calculated for each event (suffixes p and s indicate the backscattered-light polarization parallel and perpendicular to the laser one). The depolarization defined in this work differs



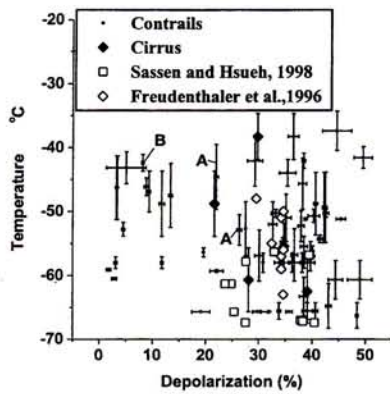


**Figure 1.** Scatter plot of the 61 contrails. The depolarisation error bars include the variability of  $\delta$  within the contrail and the effect of noise. Data of Freudenthaler *et al.* (1996) are reported for contrails of age > 2 min. Data for 6 cirrus observed at IROE are also shown.

from the definition  $(\delta' = \frac{\beta_{532s}}{\beta_{532p}})$  usually reported in other

works. The conversion formula  $\delta = \frac{\delta'}{\delta'+1}$  was used in the rest

of the paper in order to convert all the cited literature data to  $\delta$ . In most of the contrails and cirrus studied, a well-defined linear relationship between  $\beta_p(z)$  and  $\beta_s(z)$  (equivalent to a constant  $\delta$ ) was observed throughout each contrail event. A similar relation was found in contrails by Freudenthaler *et al.* (1996). In these cases,  $\delta$  was computed from the slope of the straight line fitting the  $\beta_p$ - $\beta_s$  scatter plot of each contrail. The absolute error on  $\delta$  was derived from the standard deviation of the slope. In some cases, the contrail itself showed a depolarisation that contrasted with that of the surrounding cirrus, and two lines appeared in the  $\beta_p$ - $\beta_s$  scatter plot. In these cases, the contrail depolarisation was computed by fitting the contrail part of the scatter plot.

The temperature data were taken from the daily PTU soundings of San Pietro Capofiume (44.65 N, 11.62 E), located approximately 100 km NE downstream from the LIDAR site. The maximum and minimum temperatures were noted from the contrail base and top heights between two successive soundings closest to the observation time of the contrail, and the average was taken as the mean temperature. The humidity information from the PTU data was not considered to be reliable for this type of study. The (minimum) duration of the contrails was estimated from the duration of the LIDAR event. A total of 61 contrail events was studied between July 2000 and April 2001. Six cirrus cloud events were also processed, for a comparison with the contrail results.

### 3. Results

The analysis of the LIDAR depolarisation is summarized in Fig. 1 as a function of temperature. No evident trend of depolarisation with temperature was detected. Most contrails formed a cluster with  $25\% < \delta < 45\%$ . This result matched the ground-based LIDAR observations of Sassen and Hsueh (1998), and the observations of Freudenthaler *et al.* (1996) on the aged (age > 2 min) contrails (reference data have been reported in Fig. 1 after conversion to the depolarisation definition assumed in this work).

A few cirrus measurements are also shown in Fig. 1: cirrus data fall into the main contrail cluster. This result was expected, because the size distribution of contrail particles is known to

develop into the "usual" cirrus size spectrum within 10-60 minutes after generation in saturated or supersaturated air [Schröder *et al.*, 2000]. Also, by using a scanning LIDAR, Freudenthaler *et al.* (1996) found a rapid increase in depolarisation from almost zero to typical cirrus values within a few minutes after jet emission at  $T < -60^\circ$ , and an even more rapid increase at higher temperatures. Sassen and Hsueh (1998) found an inverse trend in depolarisation with time, but depolarisation of "aged" contrails was found to be similar to that of cirrus also by these authors. The main cluster of Fig. 1 could thus be attributed to "aged" contrails, dominated by ice crystals that were larger than a few microns. This interpretation was supported by the presence in the time-height-backscatter plots of virgas or diffuse structures around the core of the majority of these contrails, and by the color ratio in the 1-2 range. The relative constancy in time and height of the contrail depolarisation (Fig. 1) shows that ice-crystal growth (such as that described by Heymsfield *et al.* (1998)) or sublimation processes, if present, were not evident in the LIDAR data. A few cases showed depolarization ratios between 45% and 50%: so high values were seldom observed in cirrus and could be attributed to the presence of large, pristine hexagonal ice columns (Del Guasta, 2001). The presence of very regular ice prisms in contrail-induced cirrus was suggested by Sussmann (1997), on the basis of enhanced halo phenomena.

A relatively small number of contrails (21% of the total) showed a depolarisation of less than 15% (Fig. 1). These cases were studied in detail; their relevant characteristics are listed in Tab. I. These contrails were arbitrarily classified into two classes.

#### 3.1. Low depolarisation contrails embedded within cirrus.

20% of the 61 studied contrails were found to be embedded within cirrus layers. Among these embedded contrails, only one showed a depolarisation higher than that of the surrounding cirrus. In 5% of the cases, the depolarisation was the same as that of the cirrus, but in 66% of the embedded contrails the depolarisation was evidently lower than in the cirrus. The colour ratio was in the 1-2 range for all embedded contrails, with the exception of those of Fig. 2, that shows a series of contrails produced at the base of a cirrus layer (reference to Fig. 1, "A" marks). The depolarisation was relatively high and constant throughout the cirrus layer, with the exception of the contrail regions, in which depolarisation was much weaker (10-20%). A similar contrast between contrail and surrounding cirrus was pointed out by Sassen and Hsueh (1998) in persistent contrails. The colour ratio  $R$  was in the 1-2 range in the background cirrus,

**Table I.** Details of the Low Depolarisation ( $\delta < 15\%$ ) Contrails.

| Date     | Base<br>Km | Thick.<br>Km. | Durat<br>min | T<br>°C | $\delta$<br>% | R    |
|----------|------------|---------------|--------------|---------|---------------|------|
| 18.07.00 | 9.9        | 0.9           | 6            | -46 ± 1 | 8.8 ± 0.42    | 1-2  |
| 18.07.00 | 9.2        | 0.75          | 4            | -43 ± 2 | 5.0 ± 3.7     | 1-2  |
| 11.09.00 | 9.4        | 1.55          | 36           | -46 ± 5 | 3.4 ± 0.004   | 1-2  |
| 11.09.00 | 9.1        | 1.12          | 12           | -46 ± 5 | 3.2 ± 0.005   | 1-2  |
| 12.09.00 | 10.6       | 0.8           | 12           | -58 ± 1 | 3.1 ± 0.29    | 1-2  |
| 12.09.00 | 11.7       | 0.21          | 7            | -59 ± 2 | 1.8 ± 0.41    | 1-2  |
| 13.09.00 | 10.6       | 0.6           | 11           | -58 ± 1 | 11.8 ± 0.25   | 1-2  |
| 13.09.00 | 9.3        | 0.84          | 8            | -49 ± 5 | 11.7 ± 0.29   | 1-2  |
| 26.09.00 | 9.7        | 0.7           | 21           | -47 ± 3 | 9.4 ± 0.21    | 2    |
| 27.09.00 | 8.9        | 1.5           | 14           | -47 ± 5 | 13.3 ± 0.35   | 2-5* |
| 29.11.00 | 8.8        | 0.65          | 16           | -42 ± 1 | 8.1 ± 0.21    | 2-4  |
| 22.01.01 | 11.6       | 0.76          | 16           | -60 ± 2 | 2.9 ± 0.48    | 1-2  |

\* noisy measurement at 1064 nm



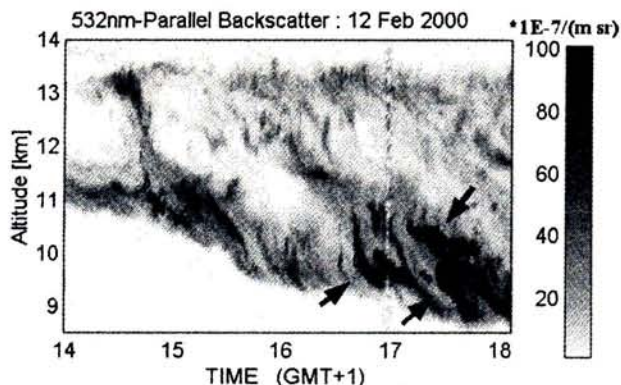


**Figure 2.** Contrails embedded into a cirrus cloud. Contrails (arrows) show a strong backscatter and a low depolarisation.

but increased up to 2-4 in the contrails. The high colour ratio and the depolarisation contrast revealed the presence of particles of different types, compared with the background cirrus. This difference was evident for the whole duration of each contrail, that was of at least 10-20 minutes. In the case of Fig.2 the visual distinction between cirrus and contrails was not always obvious, and the depolarization contrast was thus arbitrarily used to define the contrail boundaries.

The Mie theory, that is valid for spherical particles, can explain the enhanced colour ratio of fig.2 only in invoking unreasonably small (size <math><0.05 \mu\text{m}</math>) ice spheres, and cannot explain the non-negligible depolarisation observed. Ray-tracing simulations by Del Guasta (2001) showed that, when diffraction is considered, the 532 nm LIDAR depolarisation of 3-D randomly-oriented pristine ice prisms (aspect ratio >1) decreased from 50% to 15-30% when the size was decreased from 100 to 10  $\mu\text{m}$ . Ice plates showed a depolarisation below 25% for any size. The enhanced colour-ratio could be explained (in the geometric-optics approximation) by the presence of a pronounced backscatter peak in the scattering phase function, which is typical of regular hexagonal crystals: the broadening of this peak by diffraction could lead to a color ratio  $R$  up to 4 in the case of  $\sim 10 \mu\text{m}$ -sized ice crystals. The low depolarisation and the enhanced color ratio in the contrail could thus be explained by the presence of regular,  $\sim 10 \mu\text{m}$ -sized hexagonal ice crystals. Supporting this hypothesis, the presence of very regular crystals in aged contrails is considered common by several authors (e.g. Sussmann, 1997). Crystals of any type and orientation much larger than 10  $\mu\text{m}$  (like the ice plates expected to show horizontal orientation) are expected to show a lidar color ratio of 1 and thus the presence of these particles is ruled out. Schröder *et al.* (2000) showed contrail ice particles that were almost spherical in shape, and this observation makes less straightforward the interpretation of LIDAR results in terms of hexagonal crystals. Assuming that the particles are sub-spherical, the depolarisation and colour ratio of Fig.2 contrails could be explained by invoking micron-sized, spheroidal particles (Mishchenko and Sassen, 1998; Liu and Mishchenko, 2001). In particular, Liu and Mishchenko (2001) showed that a color ratio (532-1064 nm) of up to  $R=6$  is expected for randomly-oriented, almost spherical ice spheroids of  $D \sim 2-3 \mu\text{m}$ . A depolarisation in the  $\delta=10-20\%$  range is also expected for these particles. Assuming this interpretation scheme, Fig.2 would show a contrail composed of micron-sized spheroidal ice particles, like those observed by Schröder *et al.* (2000) and by Baumgardner & Gandrud (1998) in young contrails. Even if the presence of larger ice crystals cannot be ruled out on the basis of our LIDAR data, the interpretation of Fig. 2 contrails in terms of small spheroidal particles is plausible. This is because the contrails were produced in the lowest part of the cirrus where ice-super saturation is reasonably absent and particle growth probably stops in the haze mode (diameter  $D \sim 1-3 \mu\text{m}$ ), the

dominant mode in the core of precipitating contrails (Heysfield *et al.*, 1998), and in cirrus-embedded young contrails (Schröder *et al.*, 2000).

### 3.2. low depolarisation contrails without cirrus

In all, 13 contrails with low depolarisation ( $\delta < 15\%$ ) were observed (Tab.I, Fig.1) in the absence of visual or subvisual cirrus layers. The classification of these events as contrails was practically certain. The depolarisation was found to be fairly constant throughout the depth and duration of these contrails. With the exception of two cases (one of which was noisy), these contrails showed a color ratio in the 1-2 range (Tab I). The cases with  $T > -45^\circ\text{C}$  could be explained with the presence of supercooled water droplets (Pruppacher, 1995), but the possible liquid nature of colder clouds could only be explained with the presence of sulphuric acid or other solutes that lower the freezing point. However, genuine liquid cirrus-like clouds showed an almost null depolarisation (Del Guasta *et al.*, 1998), and the presence of a small, but non-null, depolarised signal is indicative of solid particles. The low color ratio and the low depolarisation could be explained by the presence of a large variety of ice and liquid particles larger than the wavelength or, alternatively, by the presence of sub-spherical, spheroidal ice particles with  $D \sim 1 \mu\text{m}$  (Liu and Mishchenko, 2001). The complete absence of cirrus clouds in the time-height-backscatter plots of 12 of the 13 low depolarisation contrails suggests that air was ice sub-saturated. In these conditions, it is unlikely that contrail particles

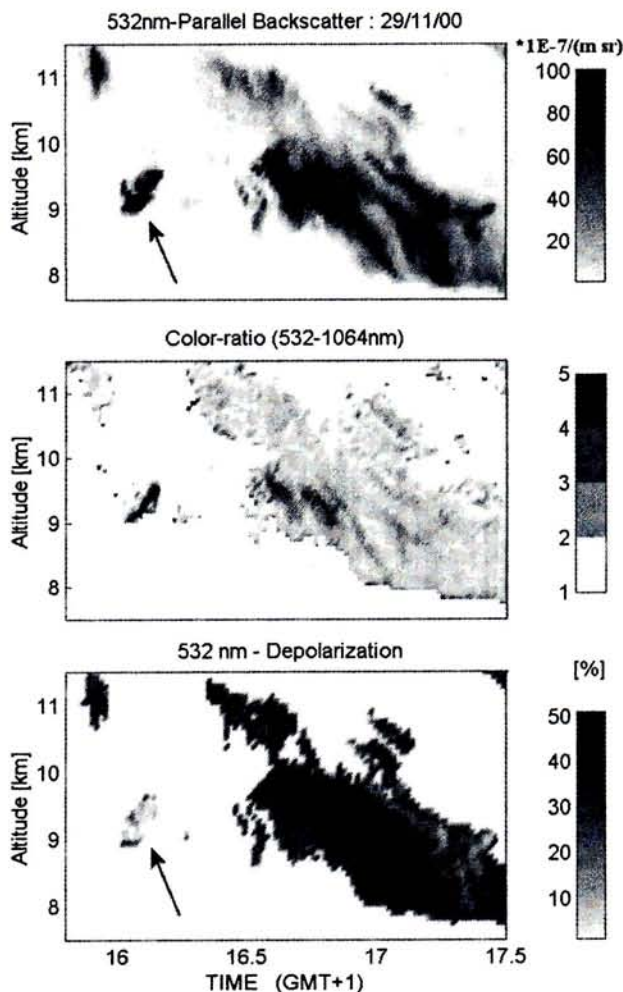


**Figure 3.** A low depolarisation contrail (arrow). Two other contrails are visible at 16:35-16:50 showing a color ratio  $R=2-4$ , and a cirrus-like depolarisation ( $\delta=30-35\%$ ).



can grow into large ice crystals, and thus the hypothesis of small, spheroidal particles is more plausible. The duration of the 13 contrails, coupled with their almost constant depolarisation, suggests that the particles did not change in size/shape within the time scale of 5-20 minutes.

In a single, unambiguous case (29/11/2000, 16 GMT+1, shown in Fig.3 and Fig.1, mark "B"), we observed a  $-42^{\circ}\text{C}$  cold contrail showing a low depolarisation ( $\delta=8\%$ ) coupled with a high colour ratio ( $R=2-4$ ) (a second contrail structure is visible in Fig.3 after 16:20, showing a depolarisation of 30-45% and an enhanced colour ratio  $R=2-4$ ). The LIDAR observation lasted 16 minutes, and the absence of a diffuse "cloud" around the contrail suggested that it was relatively young. The vertical extent of the cloud in each lidar profile was 200-400 m, and the maximum vertical span throughout the whole measurement (comparable with the height cross-section defined by Freudenthaler *et al.*, (1995)) was 600 m. This result suggests a minimum contrail age of about 15-20 min (Freudenthaler *et al.*, (1995)). The balloon-derived horizontal wind speed was 15 m/s (with almost no vertical shear); the wind direction at the cloud level was  $280^{\circ}$ , forming a small angle with the jet corridor (directed Est-West). This condition made it possible a quite long observation of the contrail, the horizontal extent of which was estimated to be in the 1-3 km range (Freudenthaler *et al.*, 1995). The closest PTU soundings showed an ice saturation ratio between 45 and 80% at the contrail level.

As in the case of Fig.2, the LIDAR results could be explained in two alternative ways: small ( $D\sim 2-3\ \mu\text{m}$ ), subspherical, spheroidal, and likely randomly-oriented ice particles (Liu and Mishchenko, 2001), or larger ice particles with a pronounced backscatter peak. If we accept the hypothesis of small, spheroidal particles (supported by the low humidity and by the in-situ observation of sub-spherical particles (Schröder *et al.*, 2000)), Fig.3 shows a contrail that does not grow into a young cirrus within the time-scale of 15-30 minutes. This time is about two magnitudes larger than the time required for the growing of large ice crystals measured by LIDAR on a jet contrail by Freudenthaler *et al.* (1996): It is also larger than the same time-scale derived for ice-saturated air by Schröder *et al.* (2000) from in-situ size distributions. Schröder *et al.* (2000) simulated the growth of contrail particles from the initial frozen stage ( $D\sim 1\ \mu\text{m}$ ) to the mature stage for different environmental conditions, showing that a large initial ice-crystal concentration, a fast contrail dilution, the absence of ice supersaturation in the surrounding air, low temperatures, and weak updraft velocities can all contribute to slowing down the crystal growth of persistent contrails. It is possible that, in these conditions, micron-sized ice particles could survive on a timescale of 15 minutes or more. The rarity of this type of contrail in our data-set could explain the absence of similar cases in the available literature.

#### 4. Conclusions

In addition to contrails that vanish within a few seconds after jet passage in dry air and contrails that rapidly develop into cirrus in ice-supersaturated air, a third type of contrail was observed that shows a low (3-20%) depolarisation. On the basis of our contrail data-set, this type of contrail was more uncommon than the "usual" contrails, i.e. those LIDAR depolarisations and colour-ratios that are indistinguishable from those of cirrus. The low depolarisation in only two cases was associated with an enhanced colour ratio in the 2-4 range. In these particular contrails, the micron-sized spheroidal particles produced at the jet passage apparently persisted in the atmosphere for more than 10-20 minutes. Unfortunately, the alternative interpretation of our LIDAR results in terms of larger, regular ice crystals cannot be definitely ruled out. The

introduction of a LIDAR depolarised channel at 1064 nm could make it possible to measure the depolarisation wavelength-dependency, expected to be a diagnostic tool for the interpretation of LIDAR results in terms of non-spherical particles (Liu and Mishchenko, 2001). More light-scattering simulations on non-spherical particles, covering particles with  $D\sim 0.1-10\ \mu\text{m}$ , are also needed in order to develop a theoretical scheme for the unambiguous classification of depolarisation LIDAR results in terms of contrail (and cirrus) microphysics.

**Acknowledgments.** One of the authors (KN) undertook this work with the support of the "ICTP-MAE Programme for Training and Research in Italian Laboratories, Trieste, Italy". The other author (MDG) acknowledges M.I. Mishchenko, the support of the Italian Space Agency (ASI) and of the Programma Nazionale di Ricerche in Antartide (PNRA).

#### References

- Baumgardner D., B.E. Gandrud, A comparison of the microphysical and optical properties of particles in an aircraft contrail and mountain wave cloud. *Geophys. Res. Lett.* 25(8), 1129-1132, 1998.
- Del Guasta M., M.Morandi, L.Stefanutti, S.Balestri, E.Kyro, M.Rummukainen, R.Kivi, V.Rizi, B.Stein, C.Wedekind, B.Mielke, R.Matthey, V.Mitev, M.Douard, LIDAR observation of spherical particles in a  $-65^{\circ}\text{C}$  cold cirrus observed above Sodankylä (FIN) during S.E.S.A.M.E., *J. Aerosol Sci.* Vol.29, 357-374, 1998.
- Del Guasta M., Simulation of LIDAR returns from pristine and deformed hexagonal ice prisms in cold cirrus by means of "face tracing", *J. Geophys.Res.* 106 ,D12 , 12589-12602, 2001.
- Freudenthaler V., F. Homburg, H.Jager, Contrail observations by ground-based scanning lidar: cross-sectional growth. *Geophys. Res. Lett.* 22, 3501-3504, 1995.
- Freudenthaler V., F. Homburg, H.Jager, Optical parameters of contrails from LIDAR measurements: Linear depolarisation. *Geophys. Res. Lett.* 23 (25), 3715-3718, 1996.
- Heymsfield A.J., L.M. Miloshevich, Relative humidity and temperature influences on cirrus formation and evolution: observations from wave clouds and FIRE II. *J. Atmos. Sci.* 52 (23), 4302-4326, 1995.
- Heymsfield A.J., Lawson R.P., G.W. Sachse, Growth of ice crystals in a precipitating contrail, *Geophys. Res. Lett.*, 25 (9), 1335-1338, 1998.
- Mishchenko M. I., L.D.Travis, D.W. Mackowsky, T-matrix computations of light scattering by nonspherical particles: a review, *J. Quant. Spectrosc. Radiat. Transfer* 55, 535-575, 1996.
- Liu L., Mishchenko M. I., Constraints on PSC particle microphysics derived from lidar observations, *J. Quant. Spectrosc. Rad. Transf.* 70, 817-831, 2001.
- Morandi M., A complete procedure for inverting backscattering LIDAR returns, Report IROE RR/GCF/92.11, pp 24, 1992.
- Mishchenko M. I., K. Sassen, Depolarisation of Lidar returns by small ice crystals: an application to contrails. *Geophys. Res. Lett.* 25 (3), 309-312, 1998.
- Pruppacher H.R., A new look at homogeneous ice nucleation in supercooled water drops, *J. Atmos. Sci.*, 52, 1924-1933, 1995.
- Schröder F., Kärcher B., C.Durore, J. Ström, A.Petzold, J.F. Gayet, B.Strauss, P.Wendling, S.Borrmann, On the transition of contrails into cirrus clouds, *J. Atmos. Sci.*, 57, 464-480, 2000.
- Sassen K., C. Hsueh, Contrail properties derived from high-resolution polarization lidar studies during SUCCESS. *Geophys. Res. Lett.* 25 (8), 1165-1168, 1998.
- Stefanutti L., F. Castagnoli, M. Del Guasta, M. Morandi, V. M. Sacco, V. Venturi, L. Zuccagnoli, J. Kolenda, H. Kneipp, P. Rairoux, B. Stein, D. Weidauer, J. P. Wolf, A Four-Wavelength Depolarisation Lidar for Polar Stratospheric Cloud Monitoring, *Appl. Phys. B*, 55, 13-17, 1992.
- Ström J., Strauss B., T.Anderson, F. Schröder F., J.Heintzenberg, P.Wendling, In situ observations of the microphysical properties of young cirrus clouds. *J. of Atmos. Sci.*, 54, 2543-2553, 1997.
- Sussmann R., Optical properties of contrail-induced cirrus: discussion of unusual halo phenomena. *Appl. Opt.* 36, 4195-4201, 1997.

Massimo Del Guasta, Istituto Ricerca sulle Onde Elettromagnetiche CNR, Via Panciatichi 64, 50127, Florence, Italy (dguasta@iroe.fi.cnr.it)  
Kandula Niranjana, Dept. of Physics, Andhra University, Visakhapatnam, 530003, India (niranjanandula@hotmail.com)

(Received June 18, 2001; revised August 17, 2001; accepted August 21, 2001.)